Measurements of Mutual Diffusivities in Concentrated Solutions of Membrane-Forming Polyamides and Cellulose Acetate

LIAO-PING CHENG,[1] AN-HWA DWAN,[2] and CARL C. GRYTE[2,*]

[1]Department of Chemical Engineering, Tamkang University, Taipei, Taiwan, Republic of China; [2]HKSM Department of Chemical Engineering, Material Science and Mining Engineering, Columbia University, New York, New York, 10027

SYNOPSIS

Mutual diffusivities at 25°C were measured in the range of the polymer weight fraction of 0.15–0.5, using differential interference microscopy. Diffusivities of atactic polystyrene in toluene at 25°C for 0.35–0.5 polymer weight fractions showed good agreement with the prediction of Vrentas and Duda. Polyamides (nylon-6, nylon-66, and a nylon-6, -66, and -610 amorphous terpolymer) in formic acid all exhibited very similar diffusivities. Although slightly higher in magnitude, the mutual diffusivities of cellulose acetate (39.8 wt % acetyl) in acetone had a compositional dependence that was parallel to the data for the polyamides. In the range of composition studied, there was an unanticipated very weak dependence of mutual diffusivity on the polymer weight fraction. © 1995 John Wiley & Sons, Inc.

INTRODUCTION

Various models[1-4] have been proposed for the unsteady-state mass-transfer processes that occur during the formation of polymeric membranes by the immersion–precipitation method. Upon direct immersion of a concentrated polymer solution ($0.05 < \phi_3 < 0.5$; ϕ_3 is the volume fraction of polymer) into a nonsolvent, a sequence of compositional changes within the membrane solution leads to the precipitation of polymer and, subsequently, the formation of a porous and/or a skinned membrane. One of the most critical parameters of the polymer solution in all of these models is the binary mutual diffusion coefficient.[1-4] Artsis et al.[5] used microinterferometry to measure the mutual diffusion coefficients over almost the entire concentration range for a variety of organic solvents in ethyl cellulose. Diffusion measurements have been made on dilute polymer solutions to determine polymer diffusivity at infinite dilution.[6-9] Other authors[10-13] characterized the effect of polymer–polymer interaction in slightly more concentrated solutions ($0.01 < \phi_3 < 0.1$). Fujita[14] and then Duda and Vrentas[15,16] developed a free-volume theory for mutual diffusion in polymeric systems over a very wide range of composition. Tirrell[17] reviewed the recent work of de Gennes and others in applying reptation to polymer self-diffusion in melts and semidilute solutions. However, very few useful measurements of the mutual diffusivity in the composition range ($0.05 < \phi_3 < 0.5$) that is useful for membrane formation have been reported.

Gouy[18] first described the shift of interference fringes in terms of the change in the refractive index with composition. Simple interferometry[19] has been used to follow diffusion in aqueous sucrose solutions,[20] agar,[21] and siloxane gels,[22] and holographic interferometry has been used in other systems to measure the diffusion coefficients.[23,24] In this work, reflected light differential interference microscopy[25-27] is used to measure the time and position dependence of compositions of acetone–cellulose acetate and formic acid–polyamide solutions in the intermediate concentration range ($0.15 < w_3 < 0.5$; w_3 is the weight fraction of the polymer). From the time evolution of the interference pattern, binary mutual diffusivity data were determined.

* To whom the correspondence should be addressed.

Journal of Applied Polymer Science, Vol. 57, 563–572 (1995)
 CCC 0021-8995/95/050563-10

EXPERIMENTAL

Two polymeric solutions with compositions 2 wt % apart are prepared and degassed. These two solutions are introduced into the fluid channel under a preadjusted microscope by slowly turning the attached micrometers (Fig. 1, see Apparatus section below for details). The fluid fronts advance at a rate of about 1 μm/s just prior to contact of the two solutions. The entire mass-transfer process was then video-recorded and then analyzed.

Apparatus

The interference cell consists of two Teflon sections (A) separated by a thin (410 microns) Teflon gasket (B), as shown in Figure 1. Solutions are introduced with micrometer-controlled syringes (C) into a thin channel (D) that is positioned between two glass windows (E and F). Glass surfaces are coated with Surfasil (Pierce Chemical Co.) to make them hydrophobic. Incident light passed through the transparent window (E), the solution channel (D), and window (F) and is then reflected back by a gold-plated mirror (G) on the lower surface of the window (F). During injection of the two liquids, trapped air is removed by two lateral grooves (H). The initial contact position between the two liquid interfaces is approximately at the same location as are the grooves (H).

The reflectance interference microscope (Peraval interphako, Jena) is capable of measuring refractive indices of small objects ($\geq$ 10 μm) with an error as small as $\pm$0.0002 refractive index units. For all experiments, an interference filter is used to obtain monochromatic light (λ = 574 μm). A microscopic refractometer slide with a known refractive index (N_{ref} = 1.51490) and a trapezoidal groove (depth of the groove, d_{ref} = 14.9357 μm) is used with the microscope to measure the refractive indices of liquids. An Abby-Spencer refractometer is also used to confirm the calibration.

Images from the microscope are recorded with a camcorder (Hitachi KP-161), a time-character generator (American Video Equipment TDCT), and a video cassette recorder (Panasonic GX4). Computer image processing is facilitated by sending video images to a frame grabber board (Targa 16+, True Vision) in an IBM compatible 386 computer.

Materials

Polyamides were obtained from commercial sources and used as received. Elvamide (8061 DuPont, intrinsic viscosity = 1.761 dL/g, M_n = 56,000) is a nylon-6, -66, -610 terpolymer. Nylon-6 (Zytel 211 DuPont, intrinsic viscosity = 1.845 dL/g, M_n = 59,000) and nylon-66 (Zytel 101 DuPont; intrinsic viscosity = 2.683 dL/g, M_n = 87,000) were obtained in pellet form. All intrinsic viscosities were measured with a Ubbelohde viscometer at 25°C in a 90% formic acid aqueous solution.[28] The Mark–Houwink constants for molecular weight calculations were k = 35.3 $\times$ 10^{-3} (mL/g), a = 0.786 for nylon-66,[28] and k = 22.6 $\times$ 10^{-3} (mL/g), a = 0.82 for nylon-6[28] and the terpolymer.

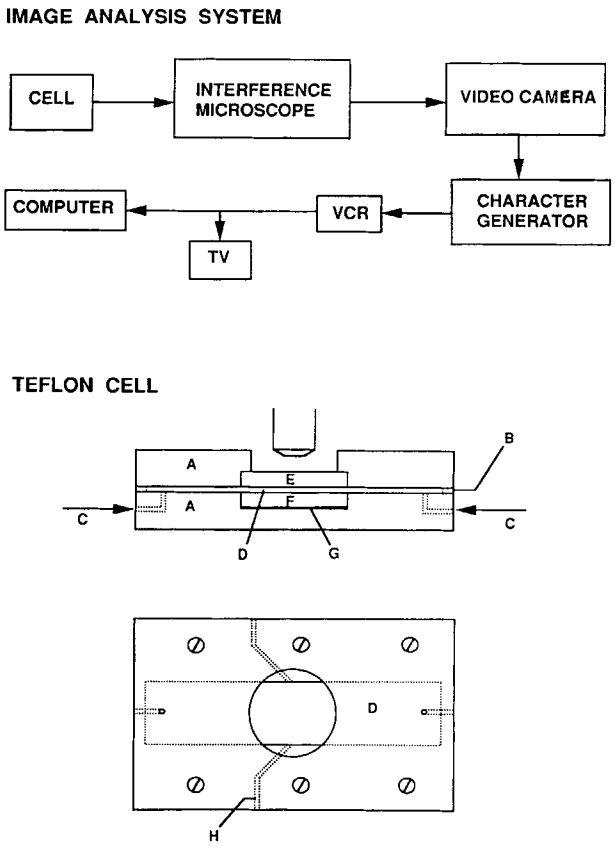

Figure 1 Schematic representation of microinterferometry apparatus: (a) data acquisition system; (b) diffusion cell.

Cellulose acetate (CA 398-3, obtained from Eastman Kodak) had an acetyl content of 39.8% and viscosity number 3 (ASTM D-1343). The number- and weight-average molecular weights were, respectively, M_n = 27,000 and M_w = 54,000.

Polystyrene (Foster Grant Co.) had a toluene intrinsic viscosity of 0.70 (dL/g). The Mark–Houwink constants for molecular weight calculations were k = 17 $\times$ 10^{-3} (mL/g) and a = 0.69 and M_n was 174,000.

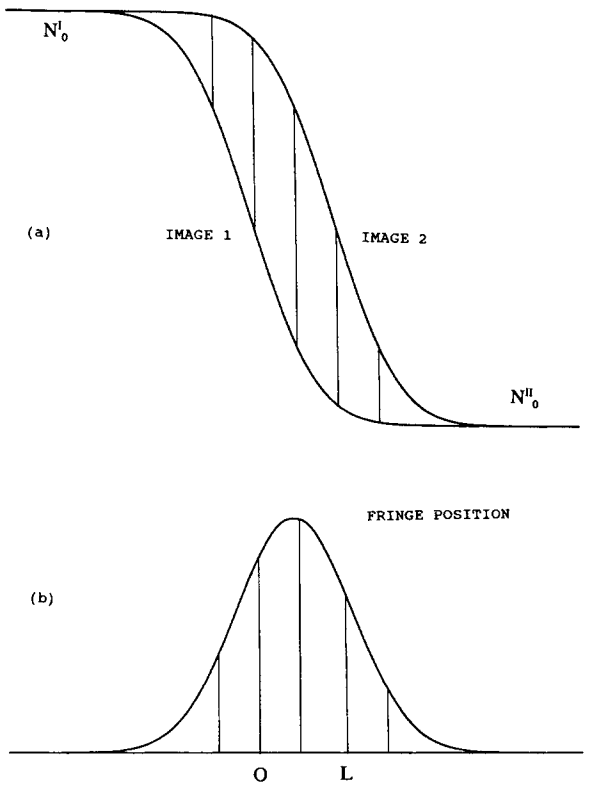

Figure 2 Refractive index variation across diffusion zone for solutions with initial refractive indices N_0^{I} and N_0^{II}: (a) image 1 shifted from image 2 by distance L; (b) fringe shift for (a).

Formic acid (purum, 98% by weight, $\rho_2 = 1.22$ g/cm^3, purchased from Fluka) was used without purification. ACS-grade acetone and toluene were from Fisher Scientific Corp. and were used without purification. Double-distilled, deionized water ($\rho_1 = 1.0$ g/cm^3) was also used.

Theory

When two isothermal solutions come in contact (as in the experiment shown in Fig. 1), one-dimensional mass transfer takes place. The diffusion equations that describe this situation are

$$\frac{\partial C_2^{I}}{\partial t} = D_{23}\frac{\partial^2 C_2^{I}}{\partial x^2} \tag{1}$$

$$\frac{\partial C_2^{II}}{\partial t} = D_{23}\frac{\partial^2 C_2^{II}}{\partial x^2} \tag{2}$$

where C_2^{I} and C_2^{II} are molar concentrations of solvent in the left- and right-hand sides of the contact interface. In writing these equations, it has been assumed that within the experimental concentration range (C_2^{I} and C_2^{II} are only slightly different), Fickian diffusion is valid and that the binary mutual diffusion coefficient, D_{23}, is constant. The suitable initial conditions for these equations are

$$C_2^{I} = C_{2,0}^{I} \tag{3}$$

$$C_2^{II} = C_{2,0}^{II} \tag{4}$$

where $C_{2,0}^{I}$ and $C_{2,0}^{II}$ are the initial concentrations. The boundary conditions are

$$C_2^{I} = C_2^{II} \qquad \text{at } x = 0 \tag{5}$$

$$\frac{\partial C_2^{I}}{\partial x} = \frac{\partial C_2^{II}}{\partial x} \qquad \text{at } x = 0 \tag{6}$$

$$C_2^{I} = C_{2,0}^{I} \qquad \text{at } x = -\infty \tag{7}$$

$$C_2^{II} = C_{2,0}^{II} \qquad \text{at } x = \infty \tag{8}$$

where the interface is defined at $x = 0$. The polymeric solution to the right-hand side of the interface has a positive coordinate, whereas the polymeric solution to the left-hand side of the interface has a negative coordinate. The analytical solution for these equations is[29]

$$C_2 = \frac{C_{2,0}^{I} + C_{2,0}^{II}}{2} + \frac{C_{2,0}^{I} - C_{2,0}^{II}}{\sqrt{\pi}} \int_0^{\frac{x}{2\sqrt{D_{23}t}}} \exp(-\eta^2)d\eta \tag{9}$$

Equation (9) is valid for solutions both in the left- and right-hand sides of the interface.

To observe the interference patterns, the Peraval interphako interference microscope applies the shearing method, in which a second image is created by shifting the original image a distance L as in Figure 2(a). These two images are then superimposed and the fringe pattern is shifted according to the spatial variation of the optical path difference between two images shown in Figure 2(b). The hypothetical concentration profile corresponding to the second image is given by

$$C_2' = \frac{C_{2,0}^{I} + C_{2,0}^{II}}{2} + \frac{C_{2,0}^{I} - C_{2,0}^{II}}{\sqrt{\pi}} \int_0^{\frac{x-L}{2\sqrt{D_{23}t}}} \exp(-\eta^2)d\eta \tag{10}$$

The fringe pattern is shifted as a result of the optical path difference between the original and the second concentration profiles:

$$C_2' - C_2 = \frac{C_{2,0}^{I} - C_{2,0}^{II}}{\sqrt{\pi}} \times \left(\int_0^{\frac{x-L}{2\sqrt{D_{23}t}}} \exp(-\eta^2) d\eta - \int_0^{\frac{x}{2\sqrt{D_{23}t}}} \exp(-\eta^2) d\eta \right) \quad (11)$$

There is a maximum point for eq. (11) at the condition $\partial(C_2' - C_2)/\partial x = 0$. It can be shown that this maximum is located at $x = L/2$ and its value is given by

$$(C_2' - C_2)_{max} = 2 \frac{C_{2,0}^{I} - C_{2,0}^{II}}{\sqrt{\pi}} \int_0^{\frac{L}{4\sqrt{D_{23}t}}} \exp(-\eta^2) d\eta \quad (12)$$

As an example, eq. (11) is computed with a hypothetical diffusion coefficient, $D_{23} = 10^{-6}$ cm/s^2, and the results are given in Figure 3. Since the two polymeric solutions have close concentrations (2 wt % apart typically), it is reasonable to assume that refractive indices of these solutions are a linear function of concentration, namely:

$$\frac{dN}{dC_2} = m \quad (13)$$

where N is the refractive index of the solution at concentration C_2 and m is a proportionality constant. Substitution of eq. (13) into eq. (12) yields

$$(N' - N)_{max} = 2 \frac{N_0^{I} - N_0^{II}}{\sqrt{\pi}} \int_0^{\frac{L}{4\sqrt{D_{23}t}}} \exp(-\eta^2) d\eta \quad (14)$$

where N_0^{I} and N_0^{II} are the refractive indices of the original solutions on the left- and right-hand sides of the interface. Calibration of the initial polymer solutions were carried out using the Peraval interphako microscope and a standard glass slide which has a known refractive index (N_{ref}) and a trapezoidal groove of precise depth (d_{ref}). N_0^{I} and N_0^{II} are related to N_{ref} and d_{ref} by eq. (15):

$$(N_{ref} - N_0^{j}) d_{ref} = K_j \lambda \qquad (j = I, II) \quad (15)$$

where $K_j (j = I, II)$ are the number of fringe shifts of the initial solutions measured with the calibration device. λ is the wavelength of the light source. Equation (15) is also applicable to the geometry of the diffusion cell of our experiment, if $N_{ref} - N_0^{j}$ is replaced by $N' - N$; d_{ref}, by d (depth of the diffusion cell, i.e., B in Fig. 1); and K_j, by K (fringe shift measured by the diffusion cell). Substitution of eq. (15) into eq. (14) yields

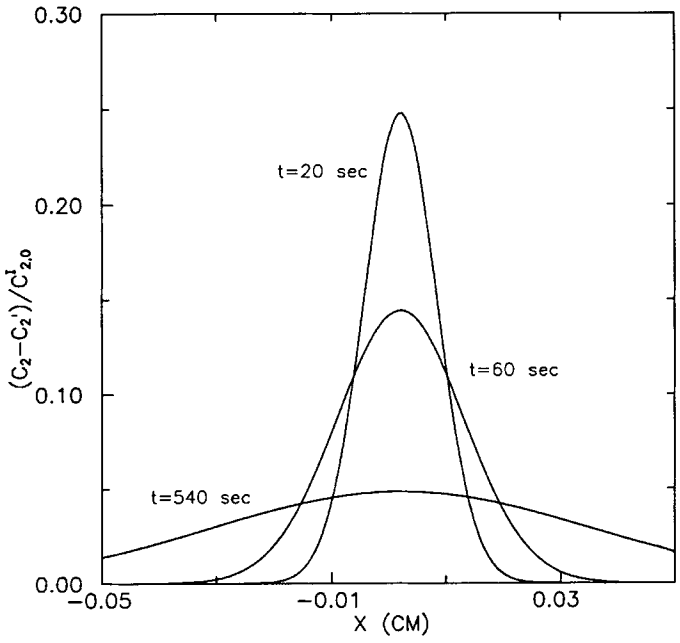

Figure 3 Fringe shift as a function of diffusion time for a hypothetical experiment, $D_{23} = 10^{-6}$ cm/s^2. Image shift, $L = 50$ μm. Solutions contact at $x = 0$.

$$\frac{K}{d} = \frac{(K_I - K_{II})}{d_{ref}} \frac{2}{\sqrt{\pi}} \int_0^{\frac{L}{4\sqrt{D_{23}t}}} \exp(-\eta^2) d\eta \quad (16)$$

Given the time and fringe shift, eq. (16) can be numerically solved[30] to obtain D_{23}.

RESULTS

Fringe Calibrations

Calibrated results of the refractive indices and the corresponding fringe shifts are shown in Figure 4 for the formic acid–nylon systems in the concentration range of interest. Refractive indices are obtained from eq. (15). By fitting with a polynomial, the number of fringe shifts for nylon-6 and nylon-66 solutions [K_6 and K_{66} in eq. (15)] are found to be related to the weight percent of the polymer (w_3) by eqs. (17) and (18):

$$K_6 = 3.82499 - 0.0446348w_3 + 0.0000474967w_3^2 \quad (17)$$

$$K_{66} = 3.83005 - 0.0456611w_3 + 0.000929648w_3^2 \quad (18)$$

For the Elvamide terpolymer, the measured refractive indices at w_3 = 15 and 32 wt % are found to be very close to those measured for the nylon-66 homopolymer (error < 0.00142%). As a result, eq. (18) is also used for the Elvamide terpolymer solutions.

Because cellulose acetate solutions are slightly translucent, precise refractive index measurements could not be achieved. Therefore, based upon the refractive index data of the two pure components, the linear relationship given in eq. (19) is assumed to be representative:

$$K_{ca} = 4.1502 - 0.0303138w_3 \quad (19)$$

For all diffusion experiments, a continuous series of interference images are recorded. In Figure 5, a typical interference pattern is given. The initial concentrations are 33 and 35 wt % terpolymer in formic acid and these images are taken at 13 s after contact. The fringe shift at the maximum point was measured to be 1.32 ± 0.02 λ. In this and succeeding images at different times, the measured maximum fringe shifts are used directly in eq. (16) to compute the diffusion coefficient, D_{23}. For a single experiment, D_{23} found for different times agreed with a precision of ±8%.

To compare with the literature results to validate our method, mutual diffusivities were also measured in the polystyrene–toluene system. The fringe shift, K_{ps}, vs. polymer weight concentration is fitted by the following equation:

$$K_{ps} = -0.14192 + 1.34655w_3 + 1.6626w_3^2 \quad (20)$$

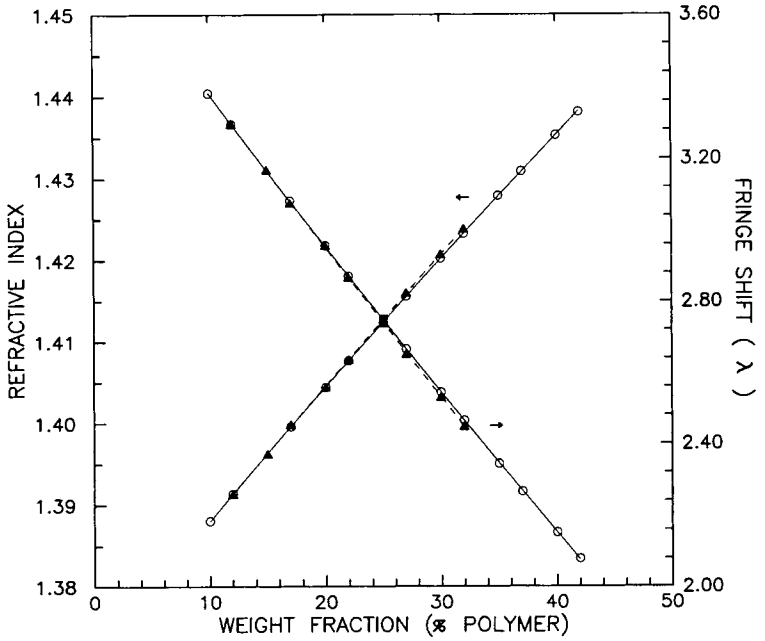

Figure 4 Calibration data for fringe shift and refractive index as a function of polymer weight fraction (wavelength λ = 574 μm): (○) nylon-6; (▲) nylon-66.

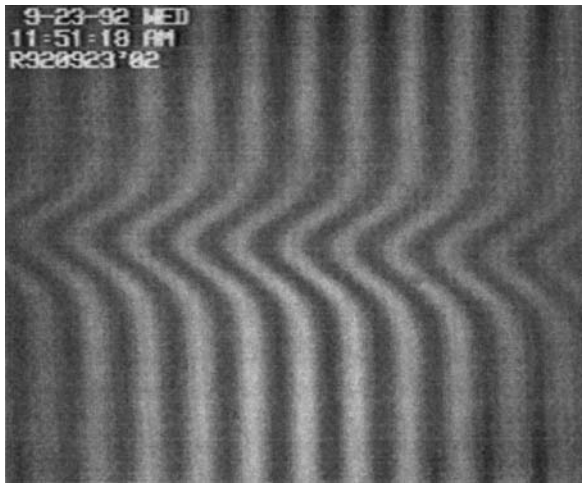

Figure 5 Image of the interference pattern for contact of nylon-66 solutions. Initial concentrations: $w^{I} = 33\%$, $w^{II} = 35\%$; $L = 50\ \mu m$; $t = 13$ s. Calculated diffusivity, $D_{23} = 3.4 \times 10^{-7}\ cm/s^2$.

Diffusion Measurements

In Figure 6, all measured diffusion data for the cellulose acetate–acetone, polyamides–formic acid, and polystyrene–toluene systems at 25°C are plotted as a function of the solvent weight fraction. The present apparatus is ideally suited to a certain range of fluid viscosities and thus the experimental window for each polymer is limited to that given in Figure 6. At low polymer weight fractions, the viscosity is not high enough to produce a stable static interface. At higher concentrations, nylon-6 and -66 are limited by their crystallization, and the Elvamide terpolymer, polystyrene, and cellulose acetate are limited by their high viscosities. The curves shown in Figure 6 are fitted results of experimental data points. During curving fitting, a two-step method is utilized: In the range of high polymer concentration (e.g., $w_3 \approx 0.9$–1.0), Duda and Vrentas's free-volume theory is employed [eq. (4) in ref. 16 for temperature at 25°C], whereas in the intermediate polymer concentration range, we apply a high-order polynomial that best matches the measured data points. This method is justified by the experimental data for cellulose acetate in acetone in this work and those of Park measured by radioactive sorption (i.e., curve *C*, see details in the Discussion) and is also justified by the observation that all measured data in the intermediate concentration range are approximately parallel. Using this curve-fitting method, curve *S* for polystyrene in toluene at 25°C is also shown in Figure 6. Since mutual diffusion coefficients for all polyamides in formic acid are similar in magnitude, they are represented by a single fitted curve, *N*.

DISCUSSION

In Figure 7, several relevant diffusion data for cellulose acetate in acetone from literature sources are shown along with the data from the present work. Park[31] measured the mutual diffusivity at very low acetone weight fractions by the radioactive sorption method. Reuvers and Smolders[3] employed a sedimentation method to measure the diffusivities in dilute cellulose acetate solutions (weight fraction of cellulose acetate < 20%). Also given in Figure 7 are the data of Artsis et al.[5] for the mutual diffusivities of ethyl cellulose in ethanol measured by an interferometric method similar to the present work. Reuvers and Smolders extrapolated their mutual diffusivity data in dilute solutions along curve M in Figure 7. This results in an exaggeration of the composition dependence of diffusivities in the intermediate composition range. Curve M is clearly divergent from the experimental data of Park and is also significantly different from the data of this report. Moreover, curve M is inconsistent in compositional dependence with the results predicted from the free-volume theory of Duda and Vrentas.[15,16] Whereas curve C has been used to successfully predict the time-dependent local composition of membrane solutions during immersion precipitation of membranes,[32] diffusivities following the compositional dependence of curve M gave unrealistic computed precipitation times (Smolders et al.[2,3] and Tsay and McHugh[4]).

In the region of polymer concentration close to 20 wt %, it is observed that mutual diffusivity data obtained from sedimentation measurements is about four times greater than that observed in this work and much larger than that anticipated by the free-volume theory.[15,16] Duda and Vrentas[15] pointed out such a discontinuity in an earlier work. The data of Artsis et al.[5] become very important, since with a single experimental method, they measured diffusivities over a very wide range of composition. Their data show no discontinuity up to a polymer concentration of 10 wt % and is consistent in compositional dependence with curve C in the intermediate range of composition.

It is useful to examine the mutual diffusivity data measured by different methods over a wide range of solvent content for atactic polystyrene. In Figure 8, experimental mutual diffusivities for the toluene–polystyrene binary system at 110°C are given as a function of polymer weight fraction. Duda and Vrentas fitted these data by using the free-volume theory, as shown by curve S-110 in Figure 8. Using the temperature shift of the free-volume theory,

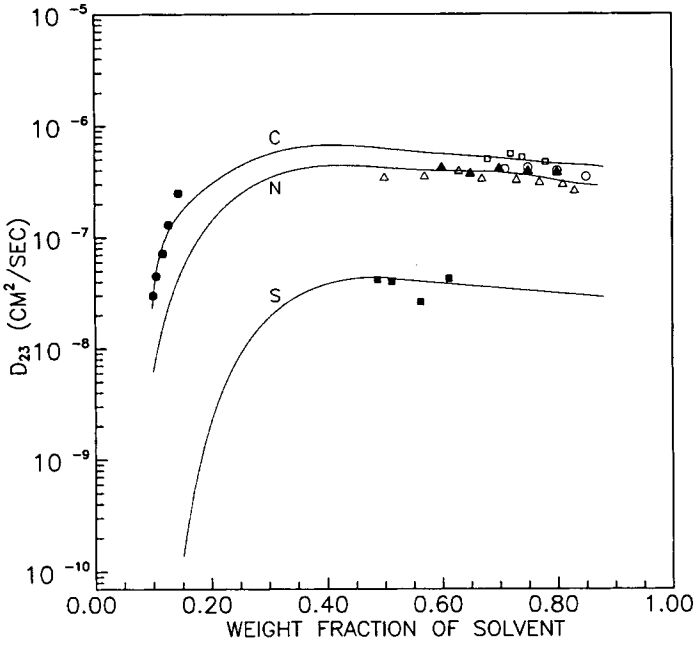

Figure 6 Mutual diffusivity as a function of solvent weight fraction at 25°C. Cellulose acetate in acetone (curve C): (□) this work; (●) data of Park[31]. Polyamides in formic acid (curve N): (○) nylon-66 in formic acid; (▲) nylon-6 in formic acid; (△) terpolymer in formic acid; (■) polystyrene in toluene (curve S).

curve S-25 is predicted for the same toluene–polystyrene system at 25°C. The present mutual diffusivity for toluene–polystyrene in the range of a 0.5–0.65 polymer weight fraction determined by microinterferometry at 25°C are also given in Figure 8. Our data appear to agree with the prediction of

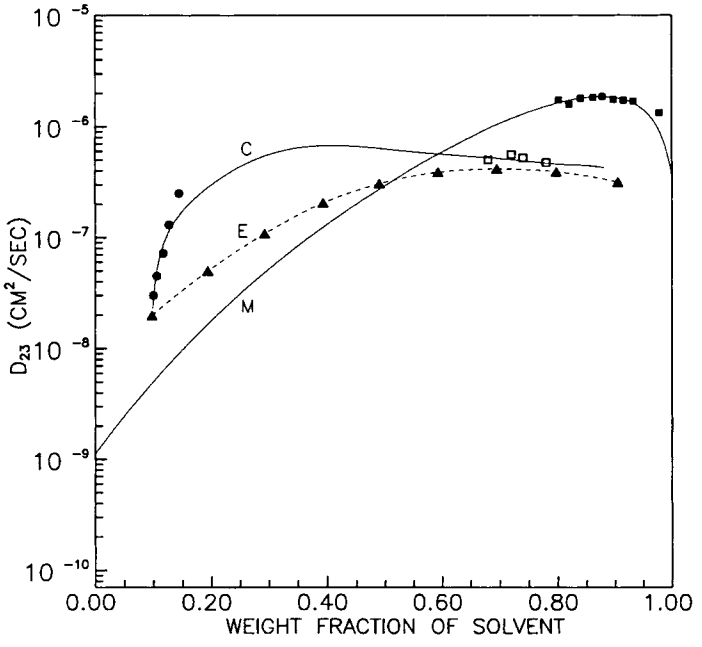

Figure 7 Mutual diffusivity as a function of solvent weight fraction at 25°C from different sources. Cellulose acetate in acetone: (■ in curve C) this work and (● in curve C) data of Park[31]; (■ in curve M) data of Smolders[3]; (▲) ethyl cellulose in ethanol[5] (curve E).

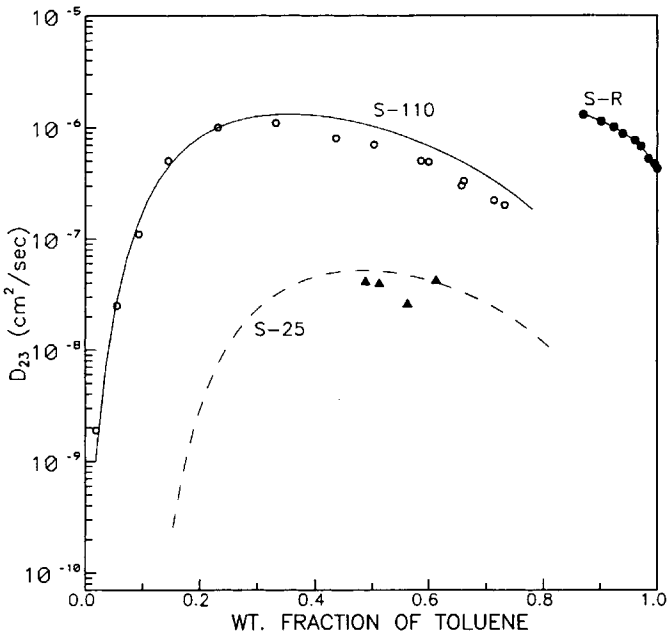

Figure 8 Mutual diffusivity of polystyrene–toulene as a function of solvent weight fraction from different sources: (▲) this work; (○) data of Duda and Vrentas[16] at 110°C (curve S-110); Duda and Vrentas's[16] prediction at 25°C (curve S-25); (●) data of Roots and Nystrom[10] (curve S-R).

Duda and Vrentas in this range of polymer composition.

Also plotted in Figure 8 are mutual diffusivities for toluene–polystyrene measured by Roots et al.[10] in the dilute range at 25°C using a sedimentation method. Just as observed by Duda and Vrentas earlier, there is a substantial and unexplained disparity between the data from sedimentation measurements and that measured by sorption methods. Other measurements in dilute solutions including polystyrene in carbon tetrachloride (Paterson et al.[33]), gelatin in water (Change and Yu[34]), polystyrene in benzene and cyclopentane, poly(ethylene oxide) in water, and dextran in water obtained by Brown[11-13] all appear to be consistent qualitatively with Roots et al. but clearly inconsistent with Duda and Vrentas and the present work.

Diffusion data may also be expressed in terms of resistance coefficients. The binary resistance coefficient, R_{23}, is defined in terms of the driving force, $\partial\mu_2/\partial x$, and the relative velocity $(u_2 - u_3)$[35,36] as

$$\frac{\partial\mu_2}{\partial x} = C_3 R_{23}(u_2 - u_3) \tag{20}$$

The resistance coefficient is related to the mutual diffusivity and the thermodynamics of the system[35] [from eq. (39) in (2)]:

$$R_{23} = \frac{\phi_2 V_3}{D_{23}} \frac{d\mu_2}{d\phi_2} \tag{21}$$

where ϕ_2 is the volume fraction of the solvent, and V_3, the partial molar volume of the polymer in the solution. In Figure 9, binary resistance data for both toluene–polystyrene and acetone–cellulose acetate systems derived from D_{23} are plotted as a function of solvent volume fraction. Curve M for cellulose acetate–acetone is computed from the D_{23} data of Smolders et al. Curve C for cellulose acetate–acetone represents the best fit of our results and the data of Park. Curve D for cellulose acetate–acetone is computed from mutual diffusivity data of toluene in polystyrene given by Duda and Vrentas that was temperature-shifted into a range appropriate to the current data at 25°C. During the calculation, a binary Flory–Huggins interaction parameter, $\chi_{23} = 0.535 + 0.11\phi_3$, is used for cellulose acetate–acetone. Also in Figure 9, Curve S-25 represents the resistance coefficient of polystyrene in toluene obtained from the Duda and Vrentas free-volume theory. Curve S is the resistance coefficient for polystyrene–toluene that corresponds to the diffusion data in Figure 6 (shown also as curve S in Fig. 6). Curve S-R represents the resistance coefficient for polystyrene–toluene

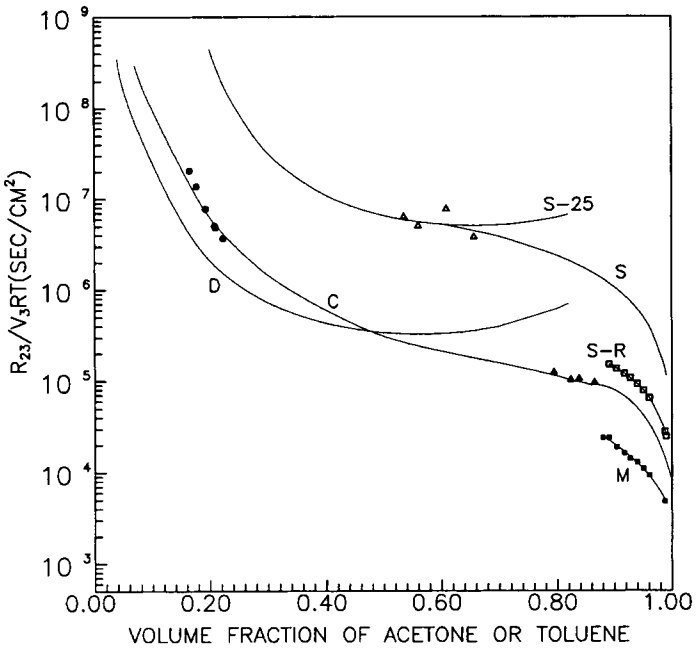

Figure 9 Binary resistance coefficients for polystyrene–toluene and cellulose acetate–acetone systems as a function of volume fraction of solvents derived from mutual diffusion data given in Figures 6–8.

computed from dilute solution sedimentation data of Roots et al.

At low solvent concentrations, the diffusivity is dominated by free-volume considerations. Park's resistance coefficient data are consistent with the predicted value of Duda and Vrentas. However, because Duda and Vrentas neglect the contribution from polymer self-diffusion,[15] the computed R_{23} for cellulose acetate–acetone at high acetone volume fractions departs very significantly from the experimental data of this work and that of Smolders et al. There appears also to be a significant difference in both the trend and the magnitude of the resistance data found by Smolders et al. from the sedimentation measurements and the current data measured by microinterferometry. Very similar inconsistencies exist when equilibrium sorption data of Vrentas and Duda[15,16] for polystyrene in toluene are compared with the sedimentation data of Roots et al.[10] These data suggest that the resistance coefficients vary sigmoidally with composition. In the concentrated range where free volume dictates and in the dilute region where polymer molecules are isolated, the resistance coefficients depend strongly on concentrations. In the intermediate range there is, however, a much weaker concentration dependence than either theory predicts.

CONCLUSION

For the polyamide–formic, cellulose acetate–acetone, and polystyrene–toluene systems, it is found that a weaker than expected concentration dependence of the mutual diffusion coefficient exists in the concentration range of $0.15 < w_3 < 0.5$.

REFERENCES

1. C. Cohen, G. B. Tanny, and S. Prager, *J. Polym. Sci.*, **17,** 477 (1979).
2. A. J. Reuvers, J. W. A. van den Berg, and C. A. Smolders, *J. Membr. Sci.*, **34,** 45 (1987).
3. A. J. Reuvers and C. A. Smolders, *J. Membr. Sci.*, **34,** 67 (1987).
4. C. S. Tsay and A. J. Mchugh, *J. Polym. Sci. Part B Polym. Phys.*, **28,** 1327 (1990).
5. M. I. Artsis, A. E. Chalykh, N. A. Khalturinskh, Yu. V. Moiseev, and G. E. Zaikov, *Eur. Polym. J.*, **8,** 613 (1972).
6. J. S. Vrentas, *J. Appl. Polym. Sci.*, **20,** 1125 (1976).
7. J. S. Vrentas, *J. Polym. Sci.*, **14,** 101 (1976).
8. C. O. Beckmann and J. L. Rosenberg, *Ann. N.Y. Acad. Sci.*, **46,** 329 (1945).
9. B. Nyström and J. Roots, *Prog. Polym. Sci.*, **8,** 333 (1982).

10. J. Roots, B. Nyström, and L.-O. Sundelöf, *Polymer,* **20,** 337 (1979).
11. W. Brown, *Macromolecules,* **17,** 66 (1984).
12. W. Brown, *Polymer,* **25,** 680 (1984).
13. W. Brown, *Polymer,* **26,** 1647 (1985).
14. H. Fujita, *Fortschr. Hochpolym.-Forsch.,* **3,** 1 (1961).
15. J. S. Vrentas and J. L. Duda, *AIChe J.,* **25**(1), 1 (1979).
16. J. L. Duda and J. S. Vrentas, *AIChe J.,* **28**(2), 279 (1982).
17. M. Tirrell, *Rubb. Chem. Tech.,* **57,** 523 (1984).
18. G. L. Gouy, *Comp. Rend.,* **90,** 307 (1880).
19. L. J. Gosting, E. M. Hanson, G. Kereles, and M. S. Morris, *Rev. Sci. Instrum.,* **20,** 209 (1949).
20. P. N. Henrion, *Trans. Faraday Soc.,* **60,** 72 (1964).
21. E. J. Schantz and M. A. Lauffer, *Biochemistry,* **1**(4), 658 (1962).
22. S. Gits-léon, F. Lefaucheux, and M. C. Robert, *J. Cryst. Growth,* **84,** 155 (1987).
23. N. Bochner and J. Pipman, *J. Phys. D Appl. Phys.,* **9,** 1825 (1976).
24. F. Lefaucheux, M. C. Robert, and Y. Bernard, *J. Cryst. Growth,* **88,** 97 (1988).
25. R. Hoffman and L. Gross, *J. Microsc.,* **91,** 149 (1970).
26. T. G. Rochow and E. G. Rochow, *An Introduction to Microscopy by Means of Light, Electrons, X-rays, or Ultrasound,* Plenum Press, New York, 1978.
27. A. D. Nikolov, P. A. Kralchevsky, and I. B. Ivanov, *J. Colloid Interf. Sci.,* **112**(1), 122 (1986).
28. J. Brandrup and E. H. Immergut, *Polymer Handbook,* Wiley, New York, 1966.
29. J. Crank, *The Mathematics of Diffusion,* 2nd ed., Oxford University Press, Ely House, London, 1975.
30. L. P. Cheng, PhD Thesis, Columbia University, New York, 1993.
31. G. S. Park, *Trans. Faraday Soc.,* **57,** 2314 (1958).
32. L. P. Cheng, A. H. Dwan, Y. S. Soh, and C. C. Gryte, *J. Polym. Sci. Polym. Phys. Ed.,* **32,** 1413 (1994).
33. G. D. Patterson, J.-P. Jarry, and C. P. Lindsey, *Macromolecules,* **13,** 668 (1980).
34. T. Chang and H. Yu, *Macromolecules,* **17,** 115 (1984).
35. P. J. Dunlop, *J. Phys. Chem.,* **68**(1), 26 (1964).
36. R. J. Bearman, *J. Phys. Chem.,* **65,** 1961 (1961).

Received August 24, 1994
Accepted September 2, 1994